

AD-A255 734



## ATION PAGE

Form Approved  
OMB No. 0704-0188

1

o average 1 hour per response, including the time for reviewing instructions, searching existing data sources, ing the collection of information. Send comments regarding this burden estimate or any other aspect of this n. to Washington Headquarters Services, Directorate for Information Operations and Reports, 1215 Jefferson of Management and Budget, Paperwork Reduction Project (0704-0188), Washington, DC 20503

DATE

3. REPORT TYPE AND DATES COVERED

Final Report

## 4. TITLE AND SUBTITLE

A Proposal to Upgrade the University of Wisconsin Volume  
Imaging Lidar

## 5. FUNDING NUMBERS

DAAL03-91-G-0222

## 6. AUTHOR(S)

E. W. Eloranta

DTIC  
ELECTE  
SEP 11 1992  
C D

## 7. PERFORMING ORGANIZATION NAME(S) AND ADDRESS(ES)

University of Wisconsin  
Department of Meteorology  
1225 West Dayton Street  
Madison, Wisconsin 537068. PERFORMING ORGANIZATION  
REPORT NUMBER

## 9. SPONSORING/MONITORING AGENCY NAME(S) AND ADDRESS(ES)

U. S. Army Research Office  
P. O. Box 12211  
Research Triangle Park, NC 27709-221110. SPONSORING/MONITORING  
AGENCY REPORT NUMBER

## 11. SUPPLEMENTARY NOTES

The view, opinions and/or findings contained in this report are those of the author(s) and should not be construed as an official Department of the Army position, policy, or decision, unless so designated by other documentation.

## 12a. DISTRIBUTION/AVAILABILITY STATEMENT

Approved for public release; distribution unlimited.

## 12b. DISTRIBUTION CODE

## 13. ABSTRACT (Maximum 200 words)

This grant provided funds to upgrade the University of Wisconsin Volume Imaging Lidar. A new computer system was purchased to increase data acquisition and data processing rates. Lidar data algorithms execute 20 to 50 times faster on the new IBM RS/6000 model 550 than on the old Digital Equipment Corp. VAX 750. The new computer has allowed us to begin systematically processing all of the 20 Gbyte data set acquired in the 1989 FIFE program. This report describes applications of the new computer.

92 9 10 012

380/60

92-24964



2494

## 14. SUBJECT TERMS

Lidar

## 15. NUMBER OF PAGES

24

## 16. PRICE CODE

17. SECURITY CLASSIFICATION  
OF REPORT

UNCLASSIFIED

18. SECURITY CLASSIFICATION  
OF THIS PAGE

UNCLASSIFIED

19. SECURITY CLASSIFICATION  
OF ABSTRACT

UNCLASSIFIED

## 20. LIMITATION OF ABSTRACT

UL

A PROPOSAL TO UPGRADE THE  
UNIVERSITY OF WISCONSIN VOLUME  
IMAGING LIDAR

FINAL REPORT

E.W. ELORANTA

MAY 1, 1992

U. S. ARMY RESEARCH OFFICE

GRANT DAAL03-91-G-0222

UNIVERSITY OF WISCONSIN  
DEPTMENT OF METEOROLOGY  
125 W. DAYTON ST.  
MADISON, WISCONSIN

APPROVED FOR PUBLIC RELEASE;  
DISTRIBUTION UNLIMITED.

DTIC QUALITY INSPECTED 1

Acquisition For	
NTIS	<input checked="checked" type="checkbox"/>
DTIC	<input type="checkbox"/>
Unpublished	<input type="checkbox"/>
Classification	
By	
Distribution/	
Availability Codes	
Dist	Avail and/or Special
A-1	

## Contents

<b>1 Abstract</b>	<b>4</b>
<b>2 Computer Installation</b>	<b>4</b>
<b>3 Scientific Applications</b>	<b>6</b>
3.1 Calculation of Wind Profiles . . . . .	6
3.2 Boundary Layer Depth Measurements . . . . .	8
3.3 Horizontal Divergence of the Boundary Layer Wind . . . . .	12
3.4 Comparison of Lidar Data with Large Eddy Simulations . . .	12
3.5 Cirrus Cloud Observations . . . . .	14
<b>4 References:</b>	<b>14</b>
<b>5 Papers published</b>	<b>15</b>
<b>6 Personal Supported</b>	<b>16</b>
<b>7 Inventions</b>	<b>16</b>
<b>8 Appendices</b>	<b>16</b>

## List of Figures

1	Volume Imaging Lidar schematic showing the previous configuration of the data acquisition system using a VAX 11/750 computer. . . . .	5
2	New configuration of the Volume Imaging Lidar data acquisition system. . . . .	7
3	A comparison of wind profiles observed with the VIL and an optically tracked radiosonde. Also included are 15 km flight leg averaged winds measured by the Canadian Twin Otter aircraft and 10 m tower winds measured NCAR PAM stations. . . . .	9
4	A time height cross section of wind speeds measured with the VIL on July 28, 1989 . . . . .	10
5	A time height cross section of wind directions measured on July 28, 1989 . . . . .	11
6	A time height cross section of the logarithm of the variance in the lidar backscatter signal measured on Aug. 28, 1989 . . . . .	13

## 1 Abstract

This grant provided funds to upgrade the University of Wisconsin Volume Imaging Lidar. A new computer system was purchased to increase data acquisition and data processing rates. Lidar data algorithms execute 20 to 50 times faster on the new IBM RS/6000 model 550 than on the old Digital Equipment Corp. VAX 750. The new computer has allowed us to begin systematically processing all of the 20 Gbyte data set acquired in the 1989 FIFE program. This report describes applications of the new computer.

## 2 Computer Installation

The University of Wisconsin Volume Imaging Lidar previously employed a VAX 11/750 computer and an attached CSPI Minimap array processor to control data acquisition and to process data(see figure 1).

This computer system was selected as the best available in 1983 when the lidar was designed. Although the VAX and Minimap were a great improvement over the PDP 11/40 used in the previous UW lidar, it imposed constraints on the VIL. Computer speed and optical disk writing rates limited the lidar pulse repetition rate to 30 Hz with no more than 1024 data points per laser profile. Three-dimensional imaging of convective layer structure was thus constrained to relatively small angular sectors ( $\sim 40^\circ$ ). The time required to scan large angular sectors became comparable to the lifetime of the atmospheric structures and wind induced motions produced large distortions of the images. Analysis of the large data sets acquired by the VIL was also very slow. It often required a week of VAX CPU time to process one hour of lidar data.

This grant provided funds to replace the VAX and Minimap array processor. The IBM RS/6000 model 550 Unix workstation purchased as a replacement is equipped with 256 megabytes of memory and 10.1 gigabytes (unformatted) of hard disk. A HP LaserJet SI laser printer and a Tektronix PhaserJet III wax phase change color printer have also been purchased to allow rapid black and white text printing and low cost, high quality, color renditions of lidar imagery. A write once optical disk (Hitachi OD321) has been ordered to provide increased data capacity (7 Gb vs 2.6 Gb) and faster data transfer speeds ( $\sim 500$  kb/s vs  $\sim 100$  kb/s).

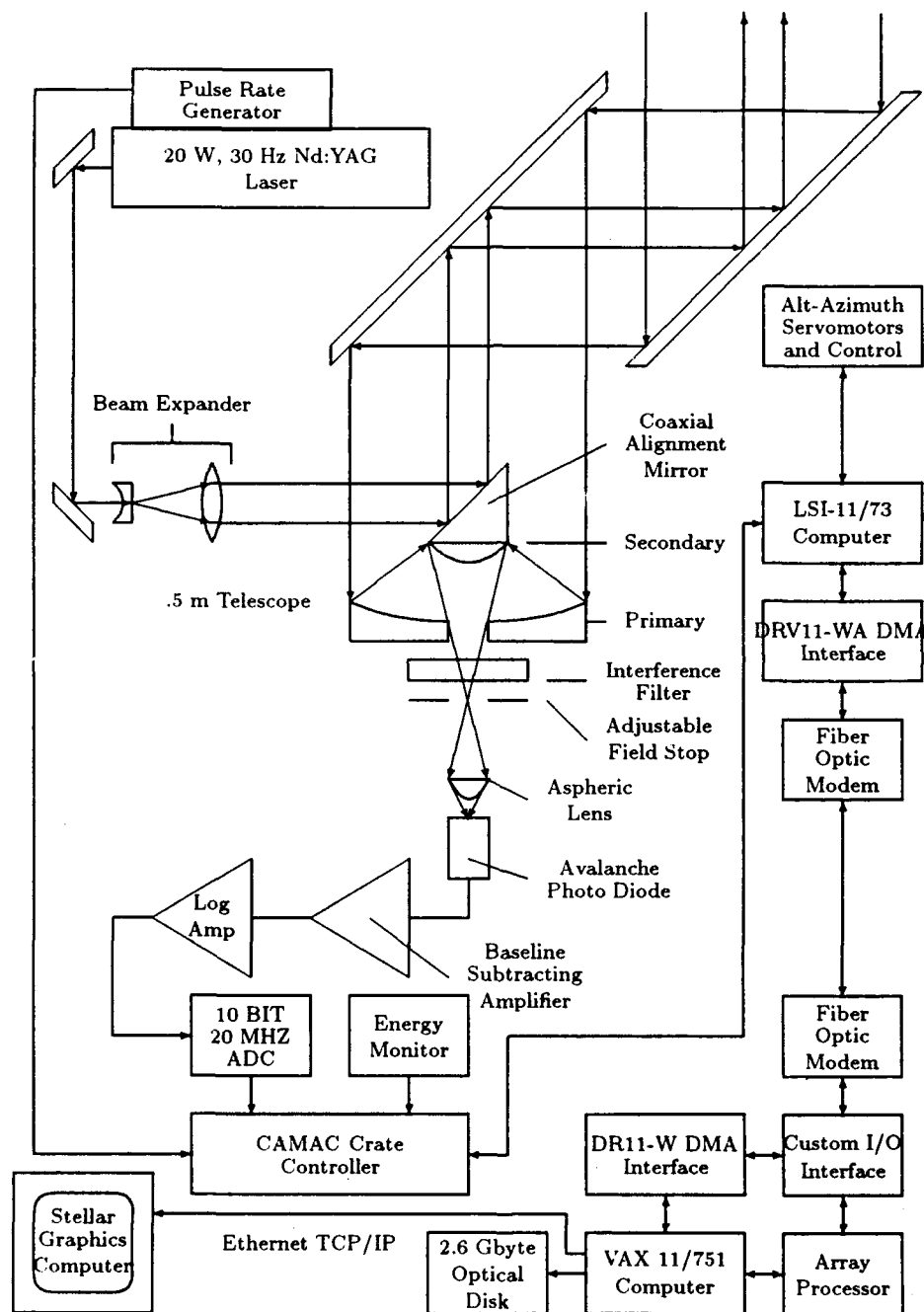


Figure 1: Volume Imaging Lidar schematic showing the previous configuration of the data acquisition system using a VAX 11/750 computer.

A 14-bit, 10 mHz word rate analog to digital converter has also been purchased to replace the 12-bit unit currently installed in the lidar. During many future experiments the additional dynamic range afforded, will allow operation without use of a logarithmic amplifier. This will eliminate subtle nonlinearities and instability problems of the logarithmic amplifier. The analog to digital convertor is now being interfaced to the VME bus of a new Intel i960 based data ingest computer which will be installed to replace the PDP-11/73 now used. The i960 has been purchased with funds from a NASA grant. The new data ingest processor along with the IBM workstation purchased on this grant will allow data transfer and recording at approximately 10 times the current rate. It should be immediately possible to operate the VIL at the 40 Hz maximum repetition rate of the current laser. Ultimately, full advantage of this capability will require purchase of a higher repetition rate laser. Figure 2 provides a block diagram of the VIL as it will be configured when all the components are installed. This can be compared to the past configuration shown in figure 1.

### **3 Scientific Applications**

This grant was limited to the purchase of new equipment and did not directly provide support for research which will employ the new hardware. However in order to illustrate the scientific impact of the grant, brief descriptions of research which will benefit from the new computer are described in this section.

#### **3.1 Calculation of Wind Profiles**

The new computer system has enabled progress in improving our algorithms for the determination of area-averaged wind velocities from the drift of patterns in the naturally occurring aerosol. Antti Piironen, a graduate student working in our laboratory, but supported by the Finnish Academy of Sciences, has refined and ported our VAX wind analysis code to the IBM computer. Wind calculations now execute approximately 50 times faster. Total throughput is still limited by the rate of data transfer from the optical disk and thus has increased by only a factor of 20. This is expected to improve when the new optical disk is installed. The increased processing speed has

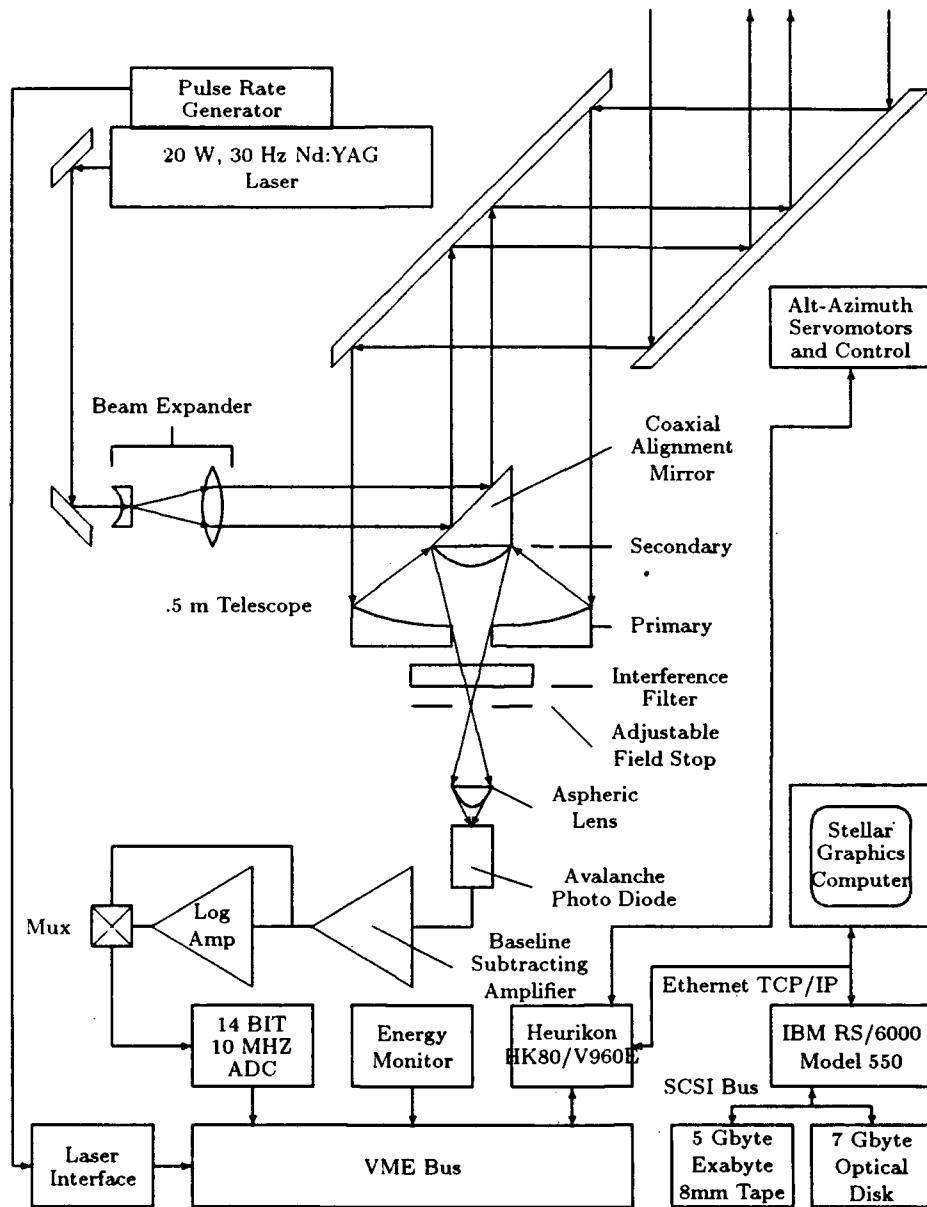


Figure 2: New configuration of the Volume Imaging Lidar data acquisition system. A IBM RS/6000 model 550 RISC workstation greatly increases data processing speeds while a Intel i960 based single board computer provides for more rapid data transfer.



allowed us to begin computing wind profiles for the entire 20 gigabyte data set acquired in the First ISLCP Field Experiment-1989 (FIFE 89). Computation of half hourly averaged vertical profiles of the horizontal wind velocity averaged over the 70km<sup>2</sup> FIFE site is now nearly complete.

Improvements to the wind algorithm have decreased random noise in the wind measurements. These improvements include: 1) the use of higher spatial resolution in computing the correlation between lidar images, 2) a better method of locating the correlation peak, and 3) careful attention to the selection of the data domain used to compute the cross correlation function. These have improved the accuracy of the measured winds and extended the range of conditions under which winds can be derived. Figure 3 shows an example of VIL winds compared with: 1) winds measured by optically tracking a radiosonde balloon, 2) aircraft wind measurements averaged over a 15 km path through the lidar scan area, and 3) the average of 8 one-hour averages of the winds measured on 10 meter tall towers arrayed over the research site. Note the exceptionally close agreement between the line averaged aircraft winds and the area averaged lidar determinations. Turbulent eddies have substantially affected the balloon measured winds so that they do not accurately reflect the area average. Also notice that even when the surface winds are time averaged over a 1 hour period the station-to-station fluctuation in the average value is large.

### **3.2 Boundary Layer Depth Measurements**

Convective layer scaling considerations (Stull <sup>1</sup>) show that the mixed layer depth is important in determining the characteristics of boundary layer turbulence. As shown by Hooper et al <sup>2</sup> variations of the magnitude of the fluctuations of lidar backscattering with altitude provide a sensitive measure of the convective boundary layer depth. Traditional radiosonde measurements of mixed layer depth are subject to large fluctuations forced by the local action of individual convective plumes. Our wind algorithms have been modified to provide the area-averaged variance in the backscatter lidar signal as part of the wind calculations. As an example of these computations figure 6 shows the logarithm of the backscatter variance plotted as a function of altitude and time. Also included in this figure are: 1) measurements of the height of the tallest convective plume, 2) the altitude at which mixed layer air covers 50% of the scan area, and 3) cloud base altitudes. These values

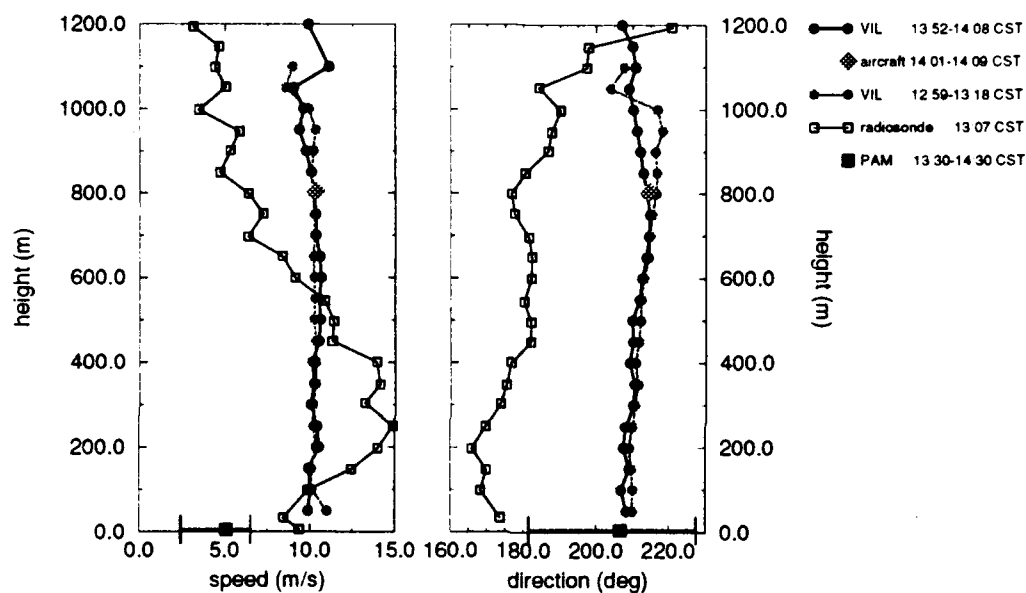


Figure 3: A comparison of wind profiles observed with the VIL and an optically tracked radiosonde. Also included are 15 km flight leg averaged winds measured by the Canadian Twin Otter aircraft and 10 m tower winds measured NCAR PAM stations. The 10 m winds are 1 hour time averages which have also been averaged over 8 separate stations close to the lidar; the error bars indicate the range of variation between station time averages. Aircraft wind measurements were provided by Mr. Ian McPherson of the National Aeronautical Establishment of Canada and the radiosonde winds by Prof. W. Brutsaert of Cornell University

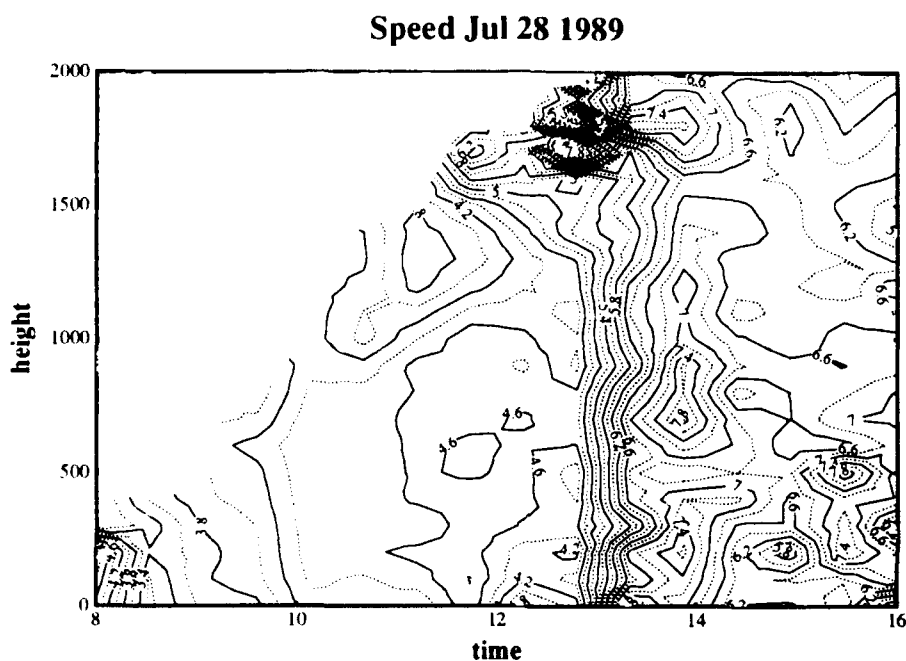


Figure 4: A time height cross section of wind speeds measured with the VIL on July 28, 1989 as part of FIFE. Wind speeds contours are shown in m/s, altitudes in m and times are CDT. This plot was prepared from 1/2 hourly profiles with 50 m vertical spacing between measurements. No additional smoothing has been applied to this plot; the area averaging inherent in these determinations have effectively averaged over turbulent fluctuations to produce a very smooth wind field. Notice the increase of wind speed from  $\sim 4.6$  to  $\sim 6.8$  m/s which occurs at 13:00 CDT. We are investigating the wind maximum shown at 13:00 CDT at an altitude of  $\sim 1700$  m: it may be an artifact caused by fair weather cumulus clouds. Figure 6 shows the altitudes of these clouds.

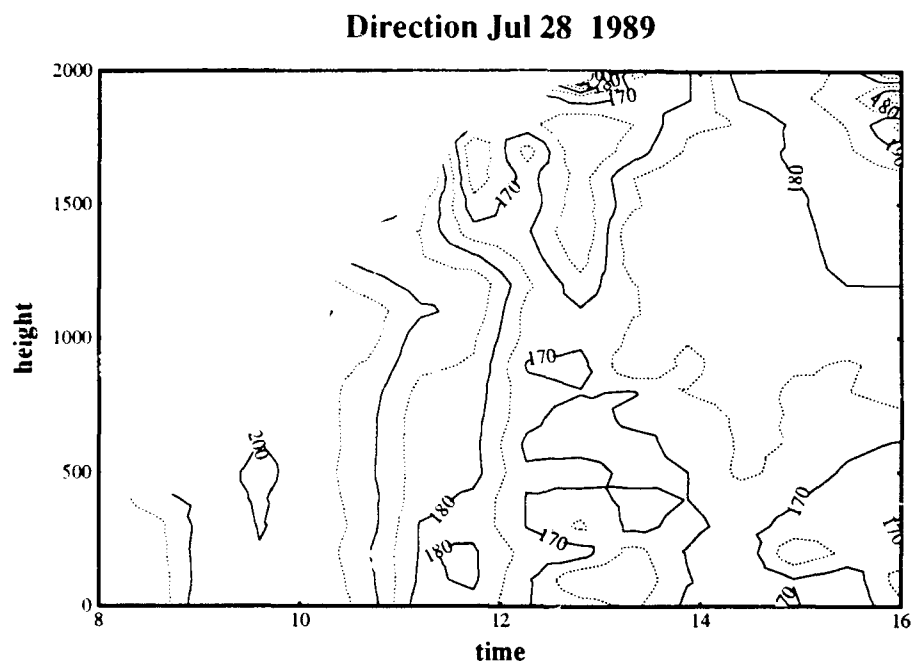


Figure 5: A time height cross section of wind directions measured on July 28, 1989 as part of FIFE. Wind direction contours are shown in degrees, altitudes in m and times are CDT. These directions correspond to speeds shown in figure 4. Notice the slow backing of the wind direction and the smoothness of the field.

were obtained by visual estimation from lidar images. Only a few of the  $\sim 1500$  images recorded each hour were sampled for the visual estimates.

### **3.3 Horizontal Divergence of the Boundary Layer Wind**

In addition to work on measuring mean winds we are pursuing efforts to compute horizontal divergence values from the lidar data. The approach we are using is described in an attached abstract submitted to the 16 th International Laser Radar Conference. Initial results of this study are encouraging. The results appear to be physically reasonable. However due to the extreme difficulty in measuring these values by other means and the limited number of cases studied, we have much work left to prove the effectiveness of these algorithms. This work has proceeded very slowly due to the fact that each determination requires repeated executions of our wind algorithms and therefore very large expenditures of computer time. This work has been performed during summers by Dr. Phil Young, a physics professor from the Plateville campus of the University of Wisconsin. This summer he proposes to move the code to the new computer; the increased computation power of the new machine is expected to greatly assist this work.

### **3.4 Comparison of Lidar Data with Large Eddy Simulations**

We have initiated a preliminary combined lidar and Large Eddy Simulation (LES) study of boundary layer structure. The computational speed, large memory and hard disk make it possible to run the LES model on the new computer.

The LES model has been modified to include a hygroscopic aerosol which can be used to predict lidar returns from modeled structures. The dependence of the backscatter intensity on relative humidity is estimated from lidar measurements. In the core of thermals air parcels have little chance to mix with air from outside of the thermal: potential temperature and water vapor content are therefore conserved as the plume core rises towards cloud base. Backscattered intensity variations observed as a function of altitude in thermal cores can then be used to derive the relative humidity dependence of the scattering for the LES simulation.

### Log Variance Jul 28 1989

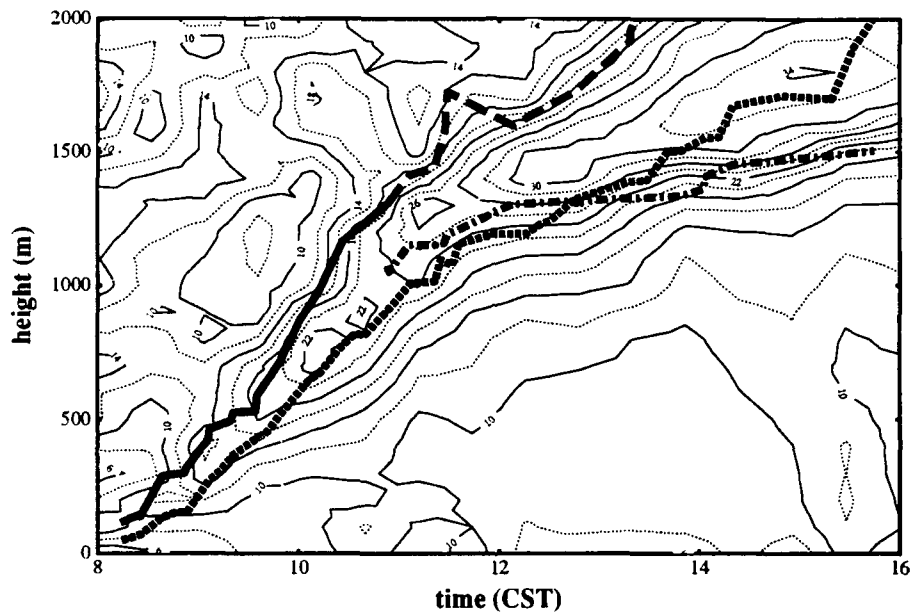


Figure 6: A time height cross section of the logarithm of the variance in the lidar backscatter signal measured on Aug. 28, 1989 as part of FIFE. For comparison, visual estimates from lidar images are also plotted for: the mean mixed layer depth (dotted line), the altitude of the highest convective plume (solid line), highest cloud echo (large dashed line) and the cloud base altitude (dashed-dot line). As shown by Hooper et al <sup>2</sup> the variance exhibits a peak value at the altitude of mean mixed layer depth. The height of the tallest plumes is also easily found from the variance plot.

LES initial conditions and surface boundary conditions have been defined for observations made during the FIFE program. A surface vegetation model has also been incorporated into the LES. The goal of this effort is to compare the predictions of the LES with the lidar observations. Comparisons will include overall boundary layer structure such as boundary layer depth and its diurnal evolution along with the spatial dimensions and spatial organization of convective plumes. Model results will also be examined to see if they reproduce spatial structures seen in the lidar data which appears to be related to surface topography.

### 3.5 Cirrus Cloud Observations

The VIL was installed near Coffeyville, Kansas between November 13 and December 7, 1991 as part of the NASA FIRE cirrus experiment. Approximately 10 Gbytes of cirrus cloud data was acquired during this period. The new computer system was installed just after this experiment and is now in service analyzing these data.

The VIL demonstrated an ability to detect cirrus clouds at ranges up to 100 km and provided routine mapping of cloud structure in a 120 km segment of sky extending 60 km on either side of the lidar. Unique images of ice particle virga falling from supercooled water clouds were obtained. In some cases ice particles fell through the freezing level; the images show a strong decrease in reflectivity as the crystals melted. Isolated ice crystal virga streamers more than 10 km long and only 100 m wide appear to indicate an isolated triggering mechanism: perhaps the action of a single ice nuclei.

## 4 References:

1. Stull, R. B., 1988: *Boundary Layer Meteorology*. Kluwer Academic Publishers, Boston
2. Hooper, W. and E. W. Eloranta, 1986: Lidar Measurements of Wind in the Planetary Boundary Layer: The Method, Accuracy and Results from Joint Measurements with Radiosonde and Kytoon, *J. of Climate and Appl. Meteor.*, **25**, 990-1001.

## 5 Papers published

- Eloranta, E. W., and D. K. Forrest, 1992: Volume Imaging Lidar Observations of the Convective Structure Surrounding the Flight Path of a Flux-Measuring Aircraft, *Accepted for publication J. of Geophysical Research*.
- Schols, J. L. and E. W. Eloranta, 1992: Calculation of Area-Averaged Vertical Profiles of the Horizontal Wind Velocity From Volume-Imaging Lidar Data., *Accepted for publication J. of Geophysical Research*.



## **6 Personal Supported**

-none

## **7 Inventions**

-none

## **8 Appendices**

Abstracts of papers submitted to the 16<sup>th</sup> International Laser Radar Conference to be held during July 1992 in Boston MA.

# Wind Profiles Derived from Volume Imaging Lidar Data: Enhancements to the Algorithm and Comparisons with Insitu Observations

Piironen, A.K., Eloranta, E.W., University of Wisconsin-Madison

This paper presents wind measurements made with the University of Wisconsin Volume Imaging Lidar (VIL) during August of 1989 as part of the First ISLSCP Field Experiment (FIFE). Enhancements to the algorithm described by Schols and Eloranta<sup>1,2</sup> are described. Comparisons of these results to aircraft, balloon and surface based wind measurements are presented. Observations of the spatial variance of aerosol backscatter are also compared to measurements of the convective boundary layer depth.

Measurements are based on two-dimensional cross correlations between horizontal image planes showing the spatial distribution of aerosol scattering observed by the lidar at intervals of approximately 3 minutes. Each image plane covers an area of 50-100 km<sup>2</sup> and the winds calculated represent area averages.

The calculation of winds from the lidar data requires several steps. In order to suppress the signal decrease as a function of range caused by attenuation, the logarithm of the energy normalized and range square corrected profiles<sup>3</sup> are first filtered using a running high pass median filter. After prefiltering, CAPPI planes are formed from the spherical coordinate VIL data. Scanning a single volume takes approximately three minutes so that image distortion caused by wind motion during the scan time must be corrected. The position of each lidar profile is adjusted by an upwind vector displacement equal to the estimated wind motion occurring in the time since the start of the scan.

A priori wind information is not necessary for this, since the correction is small and the wind calculation can be repeated by using the previous wind results as an estimated wind. Stationary aerosol sources produce fixed spatial patterns, which generate a large CCF peak at zero lag. To prevent on this, the data planes are filtered with a temporal high pass median filter.

There are often intense cloud echos in the CAPPI planes. When one of these moves in or out of the scan region between scans, the cross correlation function between planes is likely to show a strong peak due to correlation between the strong peak and a random structure in the other plane. To avoid this and to prevent correlations between single intense echos from dominating the CCF, the CAPPI planes are 'flattened' by using histogram normalization before the CCF calculation.

The cross correlation function is calculated using a Fast Fourier Transformation (FFT) on zero padded data to avoid overlaps caused by the periodicity of the Fourier

---

<sup>1</sup> Schols, J.L., Eloranta, E.W. (1990): 'The Calculation of the Horizontal Wind Velocity from Volume Imaging Lidar Data'. Accepted for publication *J. Geophysical Research*.

<sup>2</sup> Eloranta, E.W., Schols, J.L.: 'The Measurement of Spatially averaged Wind Profiles with a Volume Imaging Lidar'. *Abstracts 15th International Laser Radar Conference July 1990 Tomsk, USSR*.

<sup>3</sup> Hooper, W.P., Eloranta, E.W. (1986): 'Lidar Measurements of Wind in the Planetary Boundary Layer: The Method, Accuracy, and Results from Joint Measurements with Radiosonde and Kyttoon', *J. Climate Appl. Meteor.* 25, No 7.

Transform<sup>4</sup>. After calculation the CCF is scaled by variances of the data, giving a correlation coefficient function. The position of the CCF maximum gives the average movement of aerosols between the two scans. The CCF mass center is fitted with a quadratic polynomial surface and the maximum point of the fitted function is used to estimate the wind. This interpolates between pixel position and uses information from several pixels to improve the statistical reliability of the position estimate.

Longer time averages of the wind profiles can be done by simply averaging CCFs together. This improves the signal to noise ratio, since the random correlations average towards zero. It typically takes more than three scans for aerosol structures to move across the scan area and therefore at least two CCFs can be averaged together without significant loss in time resolution. If winds are low, we can also improve results by increasing the time separation between the scans used to calculate the CCF. If vertical resolution is not critical, vertical averaging of CCFs can also be used to increase the accuracy of the wind measurements.

Fig. 1. represents half an hour average wind profiles during  $4\frac{1}{2}$  hour measurement session on Aug 8, 1989. Much of this day exhibited very diffuse aerosol structure and thus provides a test of the wind algorithms under difficult conditions. Wind speeds and directions have been marked as • or o depending whether the correlation coefficients were larger or smaller than 0.1, respectively. Larger correlation coefficients correspond to more reliable results. The upper part of the mixed layer typically produces high contrast CAPPI images as a result of intrusions of clear air from above the mixed layer into the more turbid mixed layer: in this region correlations are almost always high. By referring to figure 3 we see that regions of low correlation and therefore less reliable results occur above the mixed layer and in the very well mixed lower middle altitudes of the afternoon profile. In regions with low correlation we still often get good answers, however, occasional spurious values appear (see for example the wind direction at 700 m in 9:30-10:00 profile).

Fig. 2. compares the VIL wind profiles to aircraft, balloon, and surface measurements. Surface measurements were generated from the average of 8 National Center for Atmospheric Studies PAM stations using anemometers on 10 meter surface towers. The aircraft measurements are Canadian NAE Twin Otter flight path averaged measurements using a Rosemount S58 gust probe to sense relative air motion and LORAN-C to provide average aircraft velocity<sup>5</sup>. We see that the results are very close to the aircraft based wind measurement. The VIL wind profiles show less noise than the optically tracked balloon based measurements: they also show a significantly different profile. This is because the balloon samples a single line through the atmosphere while the VIL provides an area average. The balloon is sensitive to individual gusts in addition to the mean wind. Comparison with PAM data shows that, as expected, the surface winds speeds are slower and the directions backed with respect to the wind aloft. Even one hour averages of the surface winds show large fluctuations between stations: the standard deviation of the 8 station averages is shown by the error bars on the surface winds.

<sup>4</sup> Press, W.H., Flannery, B.P., Teukolsy, S.A., Vetterling, W.T. (1988): 'Numerical Recipes in C, The Art of Scientific Computing', Cambridge Univ. Press. ISBN 0-521-3546-X

<sup>5</sup> MacPherson, J.I., 'NAE Twin Otter Operations in FIFE 1989', National Aeronautical Establishment of Canada. Laboratory Report LTR-FR-113

We also calculate the variance of the backscattered prefiltered lidar data displayed in each CAPPI. Fig. 3. presents the logarithmic variance of the backscatter as a function of time and altitude. For comparison we also show mean boundary layer height, cloud base, and plume tops determined by visual inspection of VIL RHI images. Convective plumes produce enhanced variance inside the mixed layer and the plume top measurements correlate very well with the boundary of this enhanced region. Another region of enhanced variance is seen before 11 am and near 2 km: this corresponds to the top of a residual aerosol layer left from the previous day's convective boundary layer. In a previous study<sup>3</sup> visual estimates of the mean boundary layer depth were found to correspond to the altitude of the lowest variance maximum. In this case the variance maximum is quite weak and appears at a slightly lower altitude than the visual estimates.

If the internal scatter in the wind profiles are used to judge the probable errors in the VIL wind determinations, we estimate accuracies of about 0.15 m/s and 2° in these profiles. The single aircraft flight leg average wind provides remarkable agreement with the VIL area average wind determination (0.2 m/s and 1 deg).

Acknowledgements: We would like to thank Finnish Academy, University of Joensuu, Finland, and Suomen Kulttuurin Edistämissäätiö Foundation for financial support to Antti Piironen, which made it possible for him to make research work in University of Wisconsin-Madison. Also NASA Grant NAG-5-902 and ARMY Research Office Grant DAAL03-86-K-0024 and DAAL03-91-C-0222 are acknowledged.

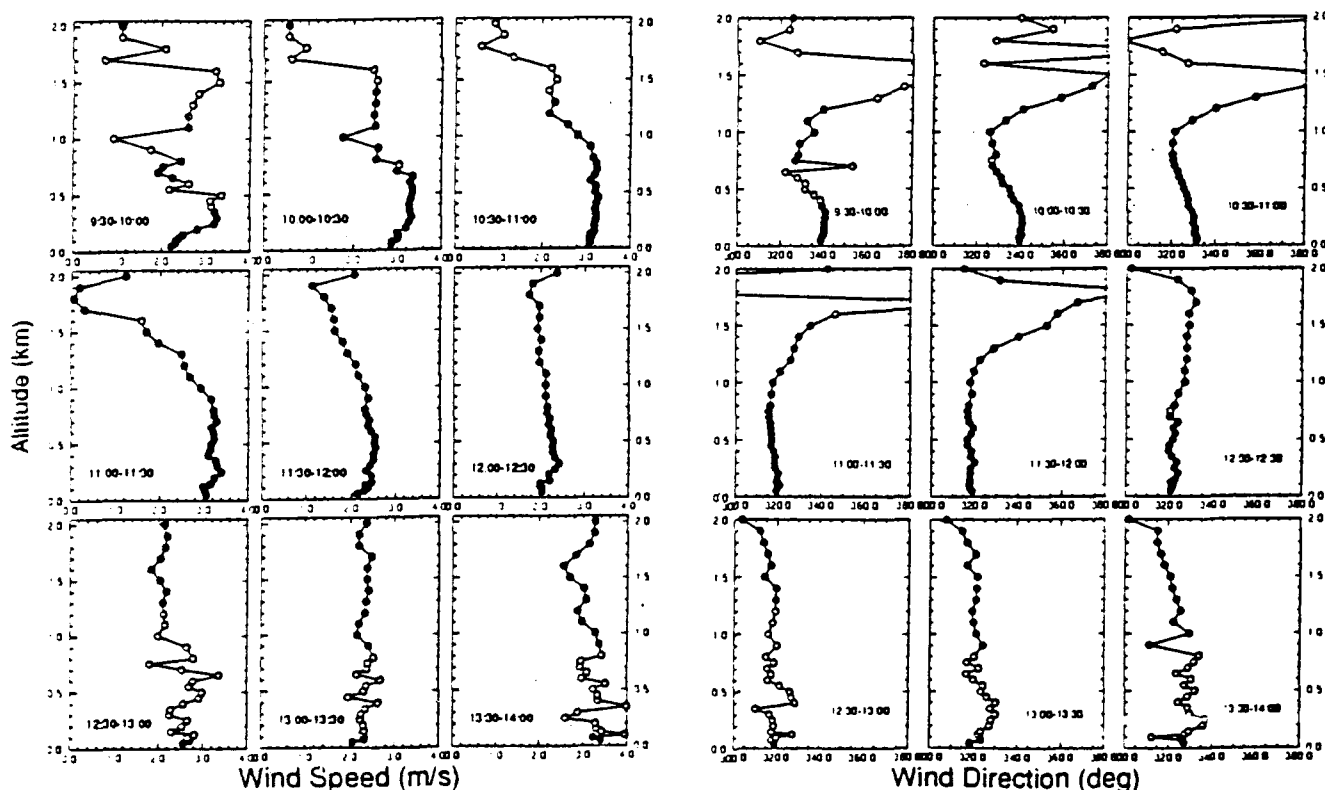


Fig. 1. VIL wind profiles between 9:30 and 14:00 on Aug 8, 1989. Open symbols indicate measurements where the correlation coefficient was smaller than 0.1.

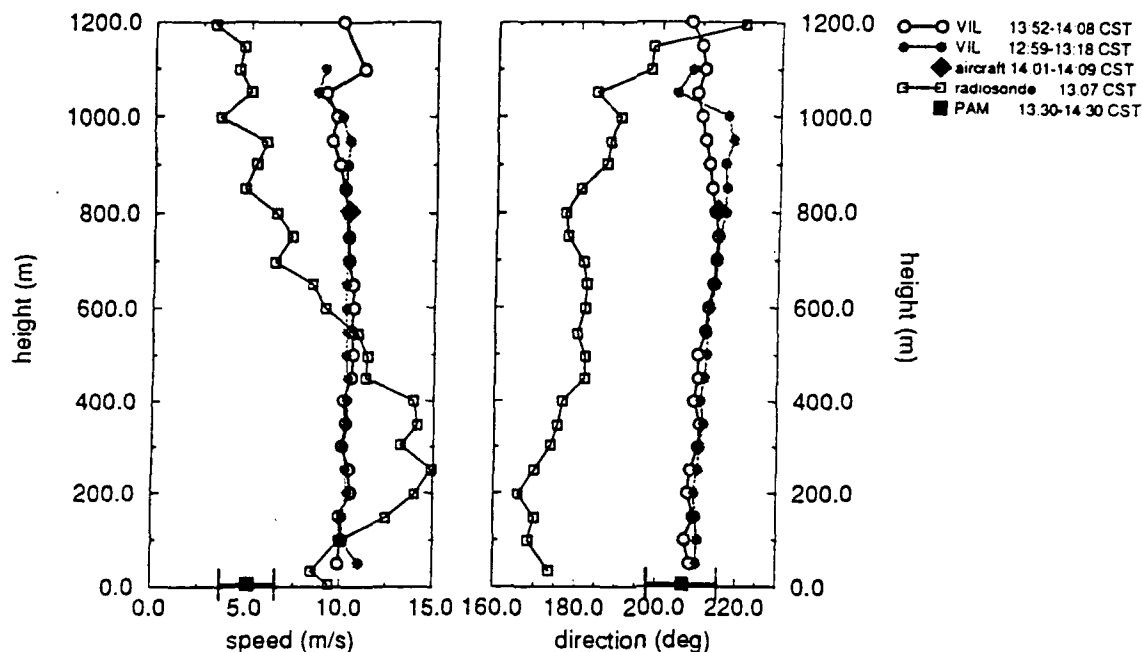


Fig. 2. Wind speed and direction measured with VIL compared to measurements made by 1) an optically tracked radiosonde, 2) aircraft instruments, and 3) anemometers on 10 meter surface towers. One hour averages of results of eight NCAR PAM stations have been used for the 10 meter measurements. Data was acquired in clear weather conditions on Aug 3, 1989.

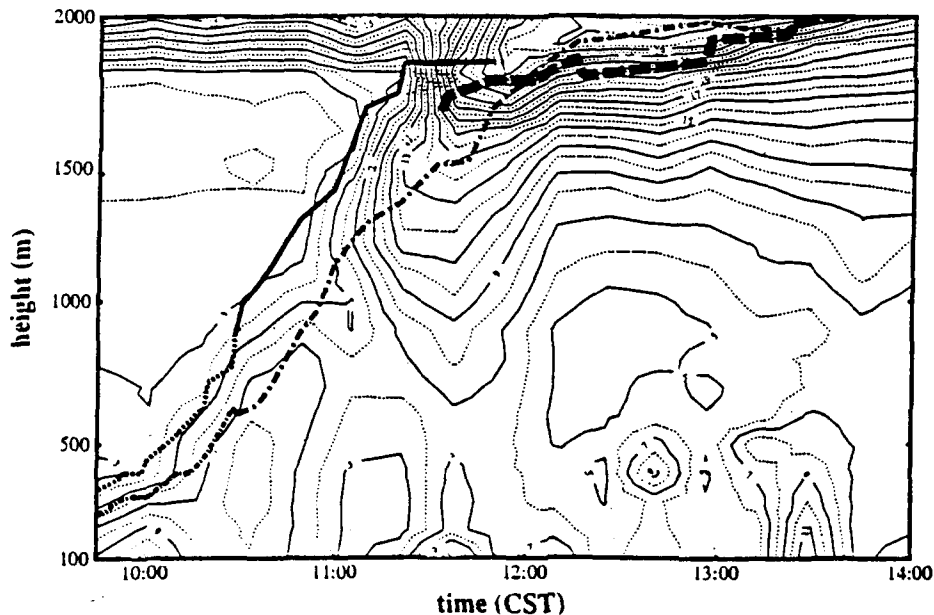


Fig. 3. Logarithmic variance of VIL CAPPI planes as a function of time at Aug 8, 1989. Plume tops are shown as continuous line. The altitude at which plumes from the mixed layer occupy 50 % of the area is shown as a dot-dashed line. Cloud base is shown as a dashed-bold line. Plume tops, mean mixed layer depth, and cloud base altitude were measured by visual inspection of VIL RHI images. The determination of boundary layer depth was difficult because of poor contrast between plumes and background before 10:30; these values are shown as shaded lines.

# MEASUREMENTS OF WIND DIVERGENCE WITH VOLUME IMAGING LIDAR

P.W. Young

Department of Physics  
University of Wisconsin - Platteville  
Platteville, WI 53818 USA

E.W. Eloranta

Department of Meteorology  
University of Wisconsin  
Madison, WI 53706 USA

Mesoscale horizontal divergence and vertical motion in the boundary layer are key ingredients in atmospheric and climate modeling. These quantities are very difficult to measure. This paper presents a technique for determining the divergence over a 10 km x 5 km area from lidar images depicting the spatial distribution of the naturally occurring atmospheric aerosols.

In the absence of sources, the temporal evolution of the spatial inhomogeneities in the atmospheric aerosol distribution is due predominantly to the wind. The mean wind translates the pattern; the spatial variations in the wind, including divergence, alter the pattern of the inhomogeneities. The University of Wisconsin Volume Imaging Lidar (VIL) produces a time sequence of three-dimensional maps of the aerosol content, thus showing the evolution of the inhomogeneities. The original line-of-sight data are first processed into horizontal sectors (typically 30° in azimuth) every 50 m in altitude. The data in each horizontal sector is then reprocessed to produce uniform, rectangular grids. These rectangular maps are then used for the divergence calculations.

The divergence is determined using the two-dimensional spatial cross correlation between successive maps in the same horizontal plane. Calculations of the mean wind from cross correlations of VIL data were first performed by Eloranta and Schols.<sup>1,2</sup> In those calculations the aerosol maps from the VIL were corrected for shape distortion caused by the mean wind over the scan time, but the effects of spatial wind variations were ignored. By taking into account at least some part of

those variations, the wind divergence can be determined from the correlation calculations along with the mean wind.

Divergence in the horizontal components of the wind velocity stretches (or compresses) the inhomogeneities in the aerosol distribution. The aerosol content in an area  $L_x \times L_y$  at the time  $t_1$  is spread into the area

$$L_x \left( 1 + \frac{\partial u}{\partial x} \Delta t \right) \times L_y \left( 1 + \frac{\partial v}{\partial y} \Delta t \right)$$

at time  $t_2$ . This spreading can be removed from the VIL map at time  $t_2$  by recalculating the horizontal data array at time  $t_2$  using this enlarged area instead of the actual area. This effectively compresses the inhomogeneities in the map back into their original shapes. The cross correlation between the actual map at  $t_1$  and the properly stretched map at  $t_2$  is greater than without this correction.

To determine the horizontal divergence, the above procedure is performed for different assumed values of  $\partial u / \partial x$  and  $\partial v / \partial y$  until the correlation is maximized. The original 10 x 5 km area, represented by a 200 x 100 array, is stretched in increments of 100 m (+50 m and -50 m) in both x and y. The VIL images are separated by approximately 3 minutes, so a 100-m stretch increment corresponds to increments of approximately  $5 \times 10^{-5} \text{ s}^{-1}$  and  $10 \times 10^{-5} \text{ s}^{-1}$  in  $\partial u / \partial x$  and  $\partial v / \partial y$ , respectively. Figure 1 shows the effects of this process on the cross correlation peak. The values for  $\partial u / \partial x$  and  $\partial v / \partial y$  are interpolated by fitting the correlation data around the maximum with a two-dimensional, second-order polynomial.

The results of this procedure for a half hour sequence at a single altitude are shown in figure 2. These data were determined from time-averaged correlation calculations, where a sequence of 5 correlations were averaged together to find the maximum. It is encouraging that the values obtained are of realistic magnitude and consistent over time, but much work remains to refine the method and verify the results.

Partial support for this work has been provided under NASA Goddard Grant NAG 5-902 and ARO Grants DAAL03-86-K-0024 and DAAL03-91-G-0222 and by a SAIF grant from UW - Platteville.

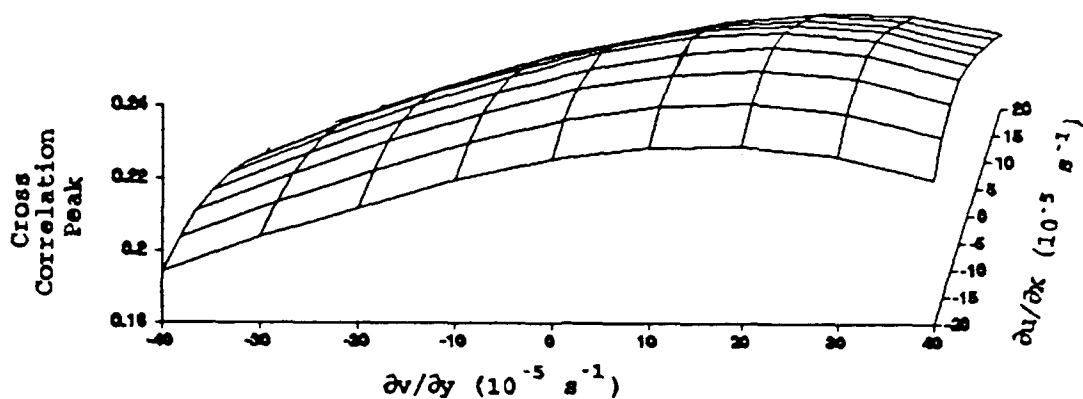


Figure 1. Cross correlation peak as a function of assumed horizontal divergence for data taken at 12:16 CDT on 8 August 1989 as part of the First ISLSCP Field Experiment (FIFE).

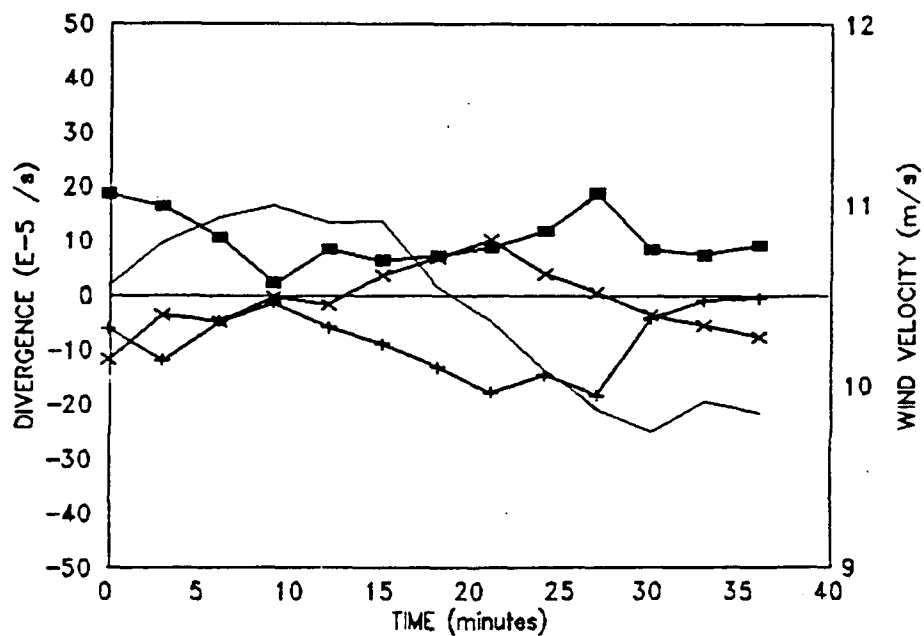


Figure 2. Divergence measurements at an altitude of 300 m starting at 11:33 CDT. Data were acquired during clear weather on 8 August 1989 as part of FIFE.  
 ..... velocity; --X--  $\partial u / \partial x$ , --+--  $\partial v / \partial y$ ; —■— divergence =  $-(\partial u / \partial x + \partial v / \partial y)$



## References

1. J.L. Schols and E.W. Eloranta, "Calculation of Area-Averaged Vertical Profiles of Horizontal Wind Velocity using the University of Wisconsin Volume Imaging Lidar Data," accepted for publication, *J. Geophys. Res.*
2. E.W. Eloranta and J.L. Schols, "Measurements of Spatially Averaged Wind Profiles with Volume Imaging Lidar," *Abstracts, 15th International Laser Radar Conference*, Tomsk, USSR, 23-27 July 1990, 227-229.